Applications of time series of microwave backscatter over the Antarctic region

Neal W Young,
and Glenn Hyland

Antarctic CRC and Australian Antarctic Division
GPO Box 252-80, Hobart, Tasmania, 7001, Australia
Phone: +61-3-62262955, +61-3-62262979, fax: +61-3-62262902
Neal.Young antcrc.utas.edu.au , Glenn.Hyland antcrc.utas.edu.au
http://www.antcrc.utas.edu.au
http://www.antdiv.gov.au

Abstract

The 500 km wide swath of the ERS Wind scatterometer and its orbit geometry allows the measurement of the microwave backscatter of all the Antarctic region between latitudes 55°S and 79°S every three days. The values of the backscatter coefficient depend on the incidence angle and look direction of the antenna beams. By removing the contributions to the backscatter of these two effects we derive normalised values of the backscatter coefficient, and from these synthesise a sequence of composite radar images of the surface. The almost continuous operation of the AMI [Active Microwave Instrument] in wind-mode provides a regular series of images commencing in August 1991.

The image sequence shows the interannual variability of melting of the surface snow cover. The increase in moisture content of the snow with warmer temperatures reduces the backscatter coefficient by as much as 25 dB below its usually very stable long term value. This signal provides a sensitive indicator of the intensity of surface melt, which is related to daily mean or maximum temperatures, as well as an estimate of the spatial extent of melting and its temporal variability.

The sequence of images clearly shows the drift of large icebergs and a major calving event from the West Ice Shelf in May 1994, which generated two very large icebergs. The first has drifted westward around Antarctica for 5000 km. The drift rate indicates a variation in speed of the westward continental slope current between 5 and 20 cm/sec. The Drift tracks of other large icebergs show the variability in the ocean current around the continent and north trending currents that link to the Antarctic Circumpolar Current further north. The backscatter from the icebergs is influenced by their surface conditions, including melting, and their size. A decrease with time in backscatter from smaller icebergs provides a measure of the reduction of their surface area by erosion.

Keywords: scatterometer, Antarctic, icebergs, melting

Introduction

Measurements of microwave backscatter from snow and ice in the Antarctic region have been made with the C-band wind scatterometer instrument deployed on the ERS-1 and ERS-2 satellites. Analysis of these measurements shows that the magnitude of the backscatter signal depends on the incidence angle of the antenna beam on the snow surface [Young et al. 1996]. The data also exhibit a directional anisotropy, such that the backscatter coefficient also depends on the look direction of the antenna beam. This directional anisotropy can be described by an amplitude and orientation which vary systematically with geographical location and surface type, i.e. continental snow cover and sea ice. The anisotropy is associated with surface roughness elements that have a preferred orientation and sub-surface snow structure formed from remnants of the surface roughness features preserved through progressive burial by the accumulating layers of snow.

Normalised backscatter values can be calculated from the data by subtracting the anisotropic contributions which can be represented by a simple formula. The normalised values represent the isotropic component of the backscatter. They are determined primarily by the bulk dielectric properties related to the crystal structure, chemical composition, and moisture content of the snow and ice. The backscatter is sensitive to changes in surface properties, particularly moisture content. Variation with time of the normalised backscatter coefficient for a given point is used to detect the occurrence of melting.

Composite images for a large area are generated by combining data from all passes within a given time interval. Each image represents the mean backscatter over that time interval. Features such as the continental margin, icebergs, and sea ice can be clearly seen in the images. The motion of objects in the ocean is also clearly visible as the displacement of features between consecutive images in a sequence. Drift tracks, speed, and the temporal variation in backscatter from the icebergs are extracted from the time series of images.

ERS-1 wind scatterometer Data

The active microwave instrument [AMI] on the ERS satellites operates at 5.3 GHz in the C-band with VV polarisation. In the wind scatterometer mode, backscatter measurements of a surface are obtained with three antennas pointing to the right of the space-craft in three directions: abeam, 45° forward, and 45° aft. The incidence angle varies across the swath from a minimum of about 18° to a maximum of about 56°. On each pass the three antennas of the instrument provide three independent observations of the surface for three different look directions at 19 regularly spaced points across the swath. Each measurement is the spatial integral of the backscatter from within the footprint of the antenna beam, an approximately circular area with a nominal diameter of 50 km. The ERS-1 satellite has been operated in three different orbit repeat cycles: 3-day (43 orbits), 35-day (501 orbits), and 168-day (2411 orbits). The maximum spacing between neighbouring ground tracks over Antarctica at latitude 65°S is about 27 km for the 35-day cycle, and about 5 km for the 168-day cycle. The ERS-2 satellite has only been operated in the 35-day repeat cycle.

We use the almost continuous sequence of backscatter measurements commencing in August 1991 from ERS-1 with a changeover to ERS-2 in June 1996, to the most recently available data in December 1996. By combining data from both ascending and descending passes we obtain multiple observations with different incidence angle and antenna look direction for any particular location within the instrument's swath. The inclination of the satellite orbit and the geometry of the scatterometer antenna system limits the backscatter observations to areas north of latitude 79°S. The 500 km wide swath of the scatterometer together with the orbit geometry allows measurement of the microwave backscatter of all the Antarctic region between latitudes 55°S and 79°S every three days.

Microwave backscatter from Antarctic snow and ice

Rott et al. [1993] showed that the microwave backscatter from the snow and ice cover over large parts of the Antarctic continent can be stable with time. Young et al. [1996] used this reported stability in the microwave properties to investigate the anisotropic character of the backscatter from the snow surface by combining data from many passes to provide measurements for a given point at multiple values of incidence angle and look direction. Figure 1 shows the variation of the backscatter coefficient as a

function of incidence angle of the measurements in July 1995. The variation with antenna beam look direction is represented by different symbols corresponding to a range of look direction. In Figure 1a the data exhibit a wide range of values for a given incidence angle, but there is a consistent pattern of largest values for look directions in the range 160° to 199°, and smallest values for 240° to 279°, with intermediate values for other look directions. For each range of look direction the variation with incidence angle is approximately linear.

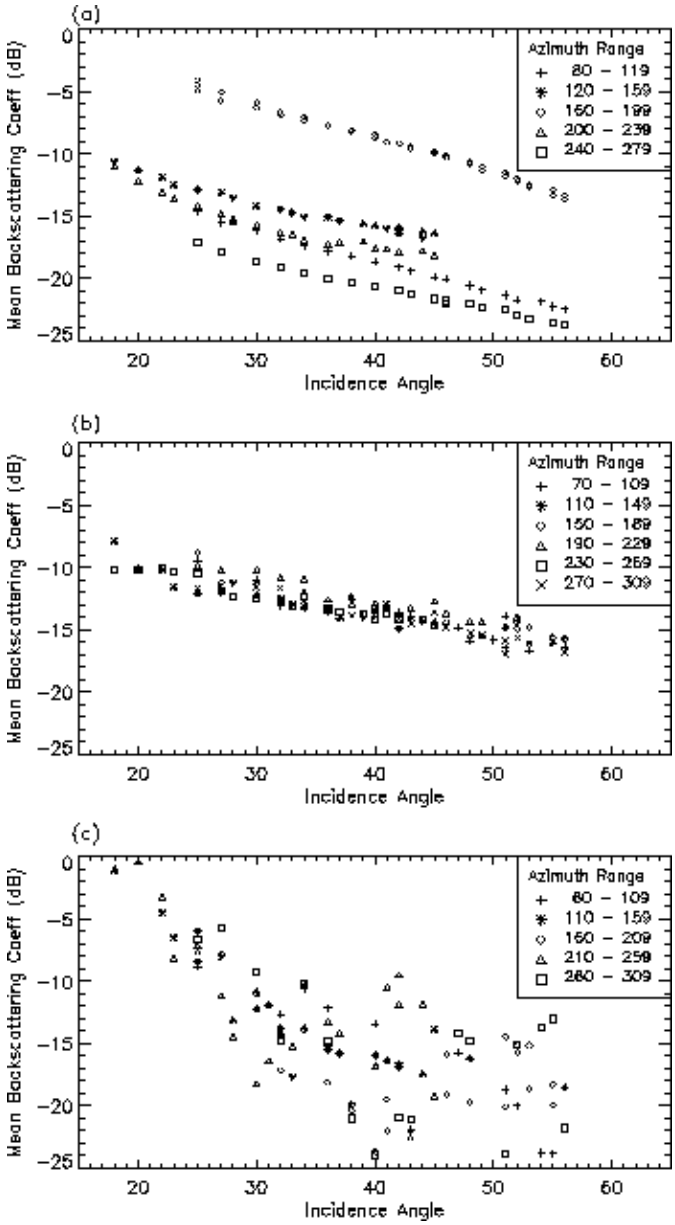

Figure 1. Mean backscatter coefficient (in dB) as a function of incidence angle illustrating the dependence on azimuth for points with three different surface types in July 1995: (a) Antarctic ice sheet in which the backscatter exhibits a strong dependence on azimuth; (b) sea ice for which the dependence on azimuth is very weak; (c) ocean where the backscatter has a quite different character to that in a or b. Each data point represents the average backscatter coefficient for a range of incidence angle of 1° and range of antenna look direction of 10°. The mean values are presented using symbols indicating a range of azimuth of 40°.

From this pattern, Young et al. [1996] showed that the backscatter coefficient for a location on the Antarctic ice sheet can be described by:

$$s = s(q0) + A\cdot(q - q0) + B\cdot\sin[2(l + f)] + e \qquad (1)$$

where

s(q0) is the mean backscatter coefficient normalised to a reference incidence angle *q0*,
q is the incidence angle of the observation,
l is the azimuth of the observation,
f is the orientation, or look direction, for minimum backscatter coefficient, and
e is the residual term.

The calculations are made for a regular array of cells 25 km square. A data value is assigned to a cell if the centre of the antenna footprint, as given in the scatterometer data product, falls within the boundaries of the cell. The normalised backscatter *s(q0)*, coefficients *A* and *B*, and the orientation term *f*, are determined for each cell through the least squares solution of equation 1 which minimises the variance of *e* for all observations assigned to that cell for a given time interval. The values of the parameters *B* (amplitude) and *f* (orientation) describe the directional anisotropy in the backscatter. They vary systematically across the ice sheet and exhibit little variation with time. The orientation of this directional anisotropy coincides with the preferred orientation of the longitudinal axis of roughness elements of the snow surface which were formed by the action of the persistent surface wind [Young et al. 1996].

The amplitude of the anisotropy over sea ice is almost everywhere small and for many purposes could be neglected (Figure 1b). This property of the backscatter from sea ice is used in setting a flag in the data product to indicate the presence of sea ice. By contrast, Figure 1c does not show a similar systematic pattern with antenna look direction in the backscatter from the ocean surface, apart from a greater dependence on incidence angle. The roughness of the ocean surface is directly related to the prevailing wind which is constantly changing in strength and direction. The solution of equation 1 almost always gives a high variance for the residual term over the ocean. The variance of the residual is typically very small for backscatter from snow and ice, which is consistent with longer-term stability of the surface roughness orientation.

Normalised backscatter coefficient

The normalised backscatter term, *s(q0)*, represents the isotropic component of the backscatter coefficient which is related to the intrinsic material properties such as the bulk dielectric constant. For each individual observation of the backscatter coefficient obtained from the satellite data stream, a normalised value, adjusted to a reference incidence angle of 30°, is calculated from:

$$s(30) = s - A\cdot(q - 30) - B\cdot\sin[2(l + f)] \qquad (2)$$

These values are used to generate composite images of the mean backscatter for the Antarctic region at regular time intervals. The orbital pattern and antenna geometry allows for a complete cover of the region every three days. However, data gaps do occur, for instance when SAR data are acquired, so a nominal interval of five days is used for the data integration. Mean values are calculated for each 25 km square cell. This process produces a series of images at five day intervals of the mean normalised backscatter over that five days.

As part of the integration process, bad data are rejected if there is a large difference from the calculated mean value. The resulting series of images provide an almost continuous record over the duration of the ERS missions. There are a few 5-day intervals for which there was little or no data provided in the data products, such as during orbital adjustment manoeuvres. Animation of this sequence has provided a valuable tool to visualise the temporal development of events.

The same procedure allows a time series to be generated at finer temporal resolution for any given cell. For convenience of analysis, mean values are calculated for each day using available data. Figure 2 shows examples of sequences from the series of daily mean values for the north-east corner of the Amery Ice Shelf (69.8°S 72.6°E). The backscatter values are exceptionally stable for the months of March through November. Excluding the summer seasons of December to February from the total series from August 1991 to December 1996 , the overall mean value of the normalised backscatter coefficient (at a reference incidence angle of 30°) is 1.22 dB and standard deviation 0.33 dB.

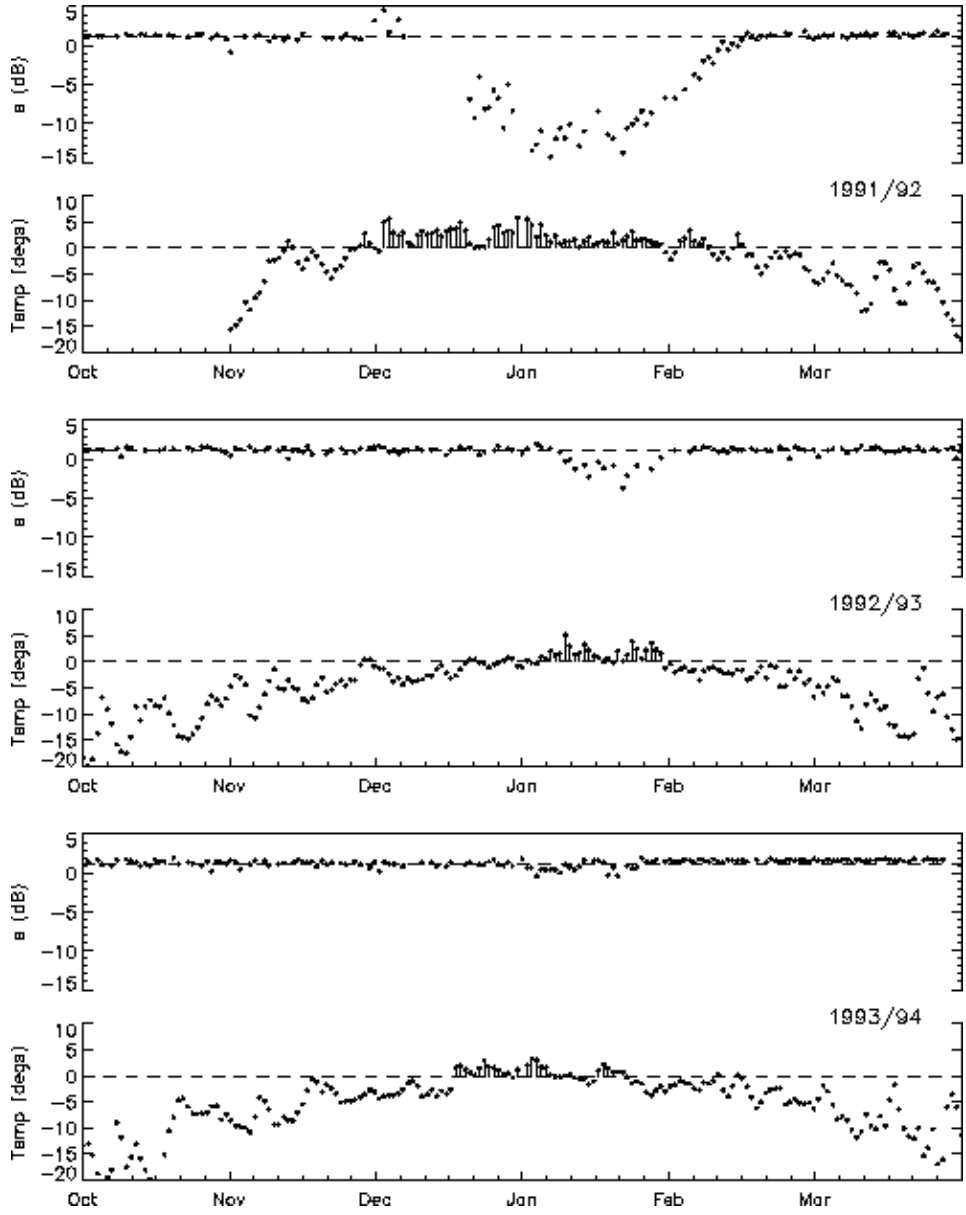

Figure 2. Time series of normalised backscatter coefficient for the north-east corner of the Amery Ice Shelf (69.8°S 72.6°E) for the months October to March for three summer seasons 1991-92 through 1993-94, and the time series of daily average air temperature at Davis station (68.6°S 78°E) in East Antarctica for the corresponding periods. The sections of the temperature series highlighted by the vertical bars indicates those periods with a mean temperature above +1°C.

Effect of snow wetness on backscatter

The presence of liquid water has a pronounced effect on the dielectric properties of snow and hence its absorption and scattering properties for microwave radiation. Rott and Nagler [1993 and 1994] showed the impact of liquid water content on the dielectric properties of snow in the European Alps, and the backscatter values observed with the SAR mode of the ERS AMI. They presented observations which indicate that a liquid water content of the near-surface snow layer of about 5% by weight causes a reduction in the backscatter by 15 to 20 dB. For dry polar snow the penetration depth at 5.3 GHz is between several metres and 20 m depending on the crystal structure of the snow and firn. Rott and Nagler [1993] derived estimates of the penetration depth using the effect of the liquid water content on the dielectric constant. The depth reduced to 138 mm with a liquid water content of 1%, and to 31 mm with 5%. This shows that as the surface snow becomes wet, backscatter will depend on the properties of the upper layer of the snow cover, and there will be a pronounced reduction in backscatter.

Figure 2 shows a significant reduction in the value of the normalised backscatter coefficient during the summer months of December to February, compared to the long term mean background value. There is considerable interannual variability in the time of onset, duration, and magnitude of this effect. In the absence of in-situ observations of snow wetness, temperature observations from the closest weather station are used. The daily mean temperatures calculated from the 3-hourly synoptic record for Davis station (68.6°S 78°E) are also presented in Figure 2. An inspection of the Figure shows that the periods when the daily mean air temperature at Davis is consistently above +1°C appear to coincide well with the intervals when there is a noticeable depression in backscatter value. This suggests that the reduction in the backscatter is indeed indicating the effect of surface thermal conditions on melting and snow wetness.

A similar correspondence is found around the Antarctic coastline between the behaviour of the backscatter for other sites and the temperature record from neighbouring weather stations. Thus the depression of the backscatter coefficient below the background value is a good indicator of snow moisture content and therefore surface melt conditions, and the magnitude of the depression is an indicator of the intensity of the melt event up to some limit where the snow is becoming saturated and the dielectric properties change to those of a wet surface.

There is not an exact correspondence between the temperature record from Davis and the backscatter record from the Amery Ice Shelf. There are two factors contributing to this. The distance between the two sites is more than 200 km allowing some difference in local thermal conditions. Secondly, the effect of surface melting on snow moisture content is cumulative while the surface remains at melting point. Thus the reduction in the backscatter will become more pronounced the longer temperature remains above a threshold level and melting continues. Meteorological records from stations distributed around the coastline show that periods with positive daily mean temperatures usually last for only a few days at a time, and occasionally for two or three weeks, so melt events are short-lived. In this case it is likely that only a shallow near-surface layer will be affected by an increase in moisture content. With a return to colder conditions, moisture will quickly freeze, and the snow becomes dry. The backscatter would then rapidly return to the background values as observed for much of Antarctica.

Figure 3 shows a set of 5-day composite images, one for each summer season from 1991-92 to 1995-96, and one for the beginning of February 1996. Each image presents the reduction in backscatter below the long term mean background value for each cell in the image, and was selected from the continuous series to show the approximate maximum melt for that season. These images provide an indication of the spatial extent of snow melt at maximum and its interannual variability. Melting always occurs over a large fraction of the Antarctic Peninsula, but with considerable variability in extent, duration, and intensity. The greatest maximum extent about the whole continent occurred in the 1991-92 summer and the least in 1994-95. The image for February 1996 shows the impact of a meteorological event that lasted just a few days late in the summer but with wide-spread effect around much of the coastline.

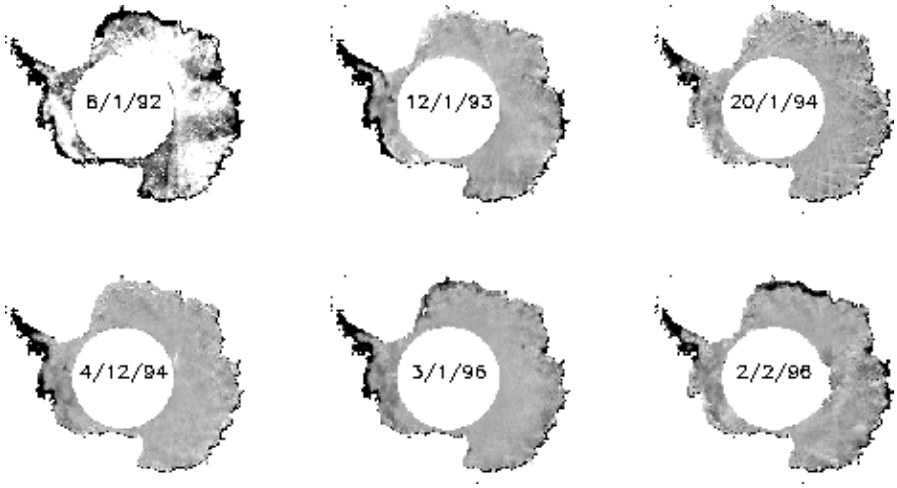

Figure 3. Spatial extent of snow wetness/melt as indicated by depression of normalised backscatter by greater than 2 dB from background values, which is represented by the dark tones, for the whole of Antarctica. Each image is a 5-day composite that was selected to represent the maximum effect for that summer season, hence an indication of the interannual variability. An additional period centred on 2 February 1996 is shown, when a short term climatic event late in the summer season had a wide-spread impact. The resolution of these images is insufficient to distinguish the high cold mountainous areas on the Antarctic Peninsula.

The greatest reductions in backscatter occur on the Antarctic Peninsula. At a site (67.1°S 61.8°W) studied by Rott et al. [1994] on the Larsen Ice Shelf on the east side of the Peninsula, the observed reduction is more than 22 dB in most summer seasons, with a maximum observed reduction of 26 dB in December 1996. The duration of the reduction in backscatter is typically several months, with the longest occurring from mid-November 1992 through late April 1993. Some melt events are short-lived and the recovery rapid over 10 to 15 days. But it is likely that with such long melt-seasons as indicated by the backscatter record there is production of substantial quantities of melt water which would percolate into the snow pack as long as it remains permeable, or collect in ponds on the surface. In this case, freezing of a considerable thickness of wet snow or bodies of water could take a long time after temperatures fall below 0°C and delay the recovery to the background backscatter value. Unfortunately no surface

temperature record is available for the site for comparison, however the observations of Rott et al. [1994] offers confirmation of these findings.

Iceberg drift tracks

The motion of very large icebergs is influenced primarily by the ocean currents. Tracking their motion in the image sequence will give an indication of mean current speed and direction averaged over the draft of the iceberg, typically 250-300 m for the icebergs in this study. Icebergs can be detected in the composite images as bright features with high backscatter amongst the relatively lower backscatter of surrounding sea ice. Two conditions cause their detection in the images to be difficult. When surrounded by open ocean, the typically high backscatter from the ocean reduces the contrast. Surface melting can reduce the backscatter from the iceberg surface to a point where it matches the surrounding surface or to an even lower value.

Figure 4 shows subsections of a sequence of composite images at ten-day intervals for the region about the West Ice Shelf. A major calving event occurred at the eastern end of the ice shelf in May 1994 when an area of 6,300 sq.km broke away from the ice shelf. The initial separation can be seen in the first frame. The section then broke into two immense icebergs in the second frame. The second iceberg (W2) remained grounded close to the ice shelf until May 1996, while the first iceberg (W1) began to drift to the west with the ocean current in frames 3 to 5.

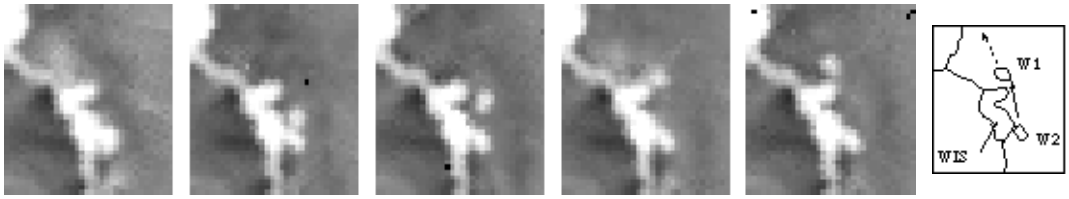

Figure 4. Sequence of images of normalised backscatter, each separated by ten days, for the region about the West Ice Shelf (WIS), East Antarctica, depicting the calving of two immense icebergs from the east end of the shelf in May 1994. The second iceberg (W2) of the pair becomes grounded a short distance from the ice shelf while the first (W1) drifts with the ocean current to the west around the Antarctic coastline. The line diagram shows the relative positions at the end of the sequence. An animated picture of the calving is also available.

Figure 5 shows various characteristics of the drift of W1 over a period of two and a half years from the West Ice Shelf to the Weddell Sea. The iceberg became grounded for short periods of up to several weeks duration at a number of locations around the coast. This can be seen in the plot of the drift speed in Figure 5c. The position in each image has been measured at the resolution of a single image cell so that the smallest observable increment of displacement is 25 km over 5 days. Also shown is the average speed calculated as the running mean over a month. Greatest speeds of up to 20 km/day and more occurred between longitudes 45°E and 25°W.

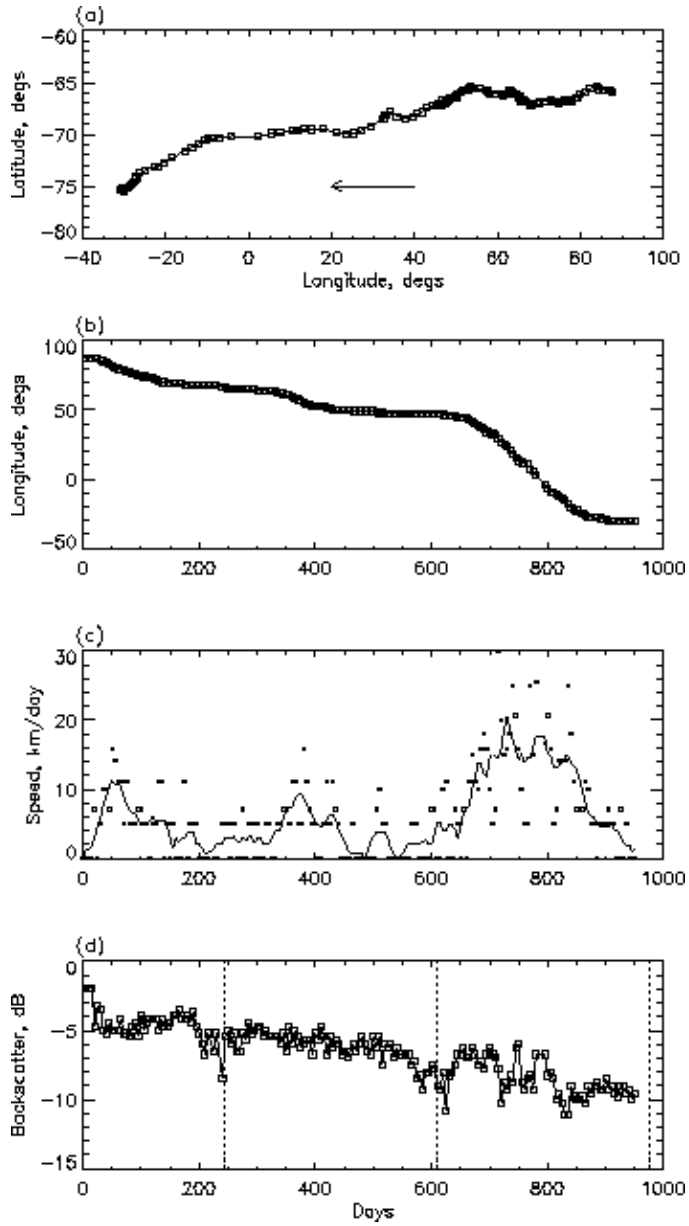

Figure 5. Characteristics of the drift of iceberg W1 from time of calving in May 1994 to end of December 1996. Measurements refer to the central pixel, usually the brightest in the feature. (a) Drift track. (b) Longitude versus time. (c) Estimate of drift speed calculated from displacement of the iceberg between consecutive 5-day composite images. The continuous curve shows the running mean of values over a 30 day interval. (d) Normalised backscatter of feature showing gradual reduction with time over the life of the iceberg.

A total of eight individual icebergs were tracked using this series of composite images. The mean backscatter values for the central pixel of all the features are mostly within the range -3 dB to -12 dB. Figure 6 shows the backscatter record for the largest of the icebergs (area 8,200 sq.km) and with the longest record. There is a marked reduction in the backscatter at several discrete intervals corresponding to four summer seasons. For the other two summers there is an insignificant change in backscatter. The reduction in backscatter is caused by strong surface melting. At the end of the summer the backscatter recovers to a value larger than immediately before the onset of melting. Between melt events there is a gradual reduction in backscatter. This can be explained by a change in crystal size within the upper snow layer. Crystal size of newly deposited snow is generally small. Refreezing of melt water in old snow usually leads to the growth of large crystals whose size can be a significant fraction of the radar wavelength and thus produce a stronger backscatter. After the end of a melt event progressive snow falls will gradually bury the old snow with finer-grained material, attenuating the backscatter so that it gradually decreases until the next melt event.

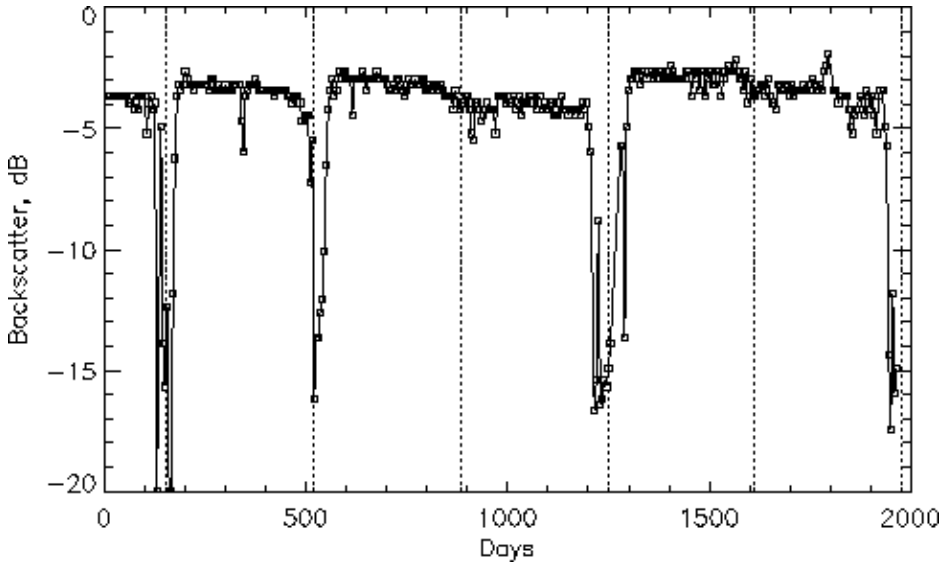

Figure 6. Time series of normalised backscatter values for iceberg B10 in the Bellingshausen Sea showing strong reduction with time corresponding to melt events in summer seasons of 1991-92, 1992-93, 1994-95, and the beginning of 1996-97 summer. At the end of each melt season the backscatter recovers to a value above that immediately before the onset of melting. There is a gradual reduction in backscatter between melt events. The vertical bars indicate the end of each calendar year.

Figure 5d shows the backscatter values over the life of the W1 iceberg. There is some evidence of a small amount of surface melting during two summers, within a gradual decrease in backscatter from -4 dB to -10 dB It is unlikely that the continued deposition of snow onto the surface has led to the observed reduction. The iceberg had a backscatter value of about -4.5 dB and an area soon after calving close to 1,740 sq.km (approximately 68 km x 34 km) which was determined from a medium resolution AVHRR image. This size is comparable to the footprint of the scatterometer beam. It is likely that the reduction in backscatter is mostly associated with gradual fragmentation and erosion of the margins of the iceberg leading to a decrease in area. Where the size of an iceberg is comparable or smaller than the footprint of the scatterometer beam, the backscatter will be an area weighted average of the backscatter from the iceberg and from some portion of its immediate environment. One of the smaller icebergs with an area of 230 sq.km has a backscatter value of -9.5 dB against a background value of -11.3 dB from surrounding sea ice. Using the measurements from the smaller berg and from W1 early in its life as calibration points, a weighted value of the backscatter from W1 and the sea ice gives an estimate of area at the end of the drift track of about 550 sq.km or 30% of the original size. This is probably a lower limit because it assumes that the surface of W1 has retained similar backscatter properties over most of its life as it had at the time of calving. This is likely since its path has remained close to the coast and it has suffered little surface melting.

The tracks of the eight icebergs are shown in Figure 7. Close to the coast their drift is to the west with the westward continental slope current, also known as the Antarctic East Wind Drift, This current appears to be constrained close to the upper edge of the continental slope. The tracks of several of the icebergs exhibit a retroflection so that they are carried northward and eventually join the eastward motion of the southern part of the Antarctic Circumpolar Current. This pattern of iceberg drift and the speeds are consistent with the findings of Tchernia and Jeannin [1984]. They used transponders deployed on 21 icebergs to measure their drift track and speed for periods up to 2.5 years. Figure 7 shows tracks around the East Antarctic coast of the first icebergs that have been observed to continue drifting to the west past a retroflection between about 80°E and 90°E described by Tchernia and Jeannin [1980] indicating the continuity of the slope current through this area. The retroflection in the western Bellingshausen Sea at about 130°W is also an additional finding. The distribution of sea ice can also be clearly seen in the composite images. There was no obvious association between the observed drift speed and the presence or absence of pack ice about the icebergs.

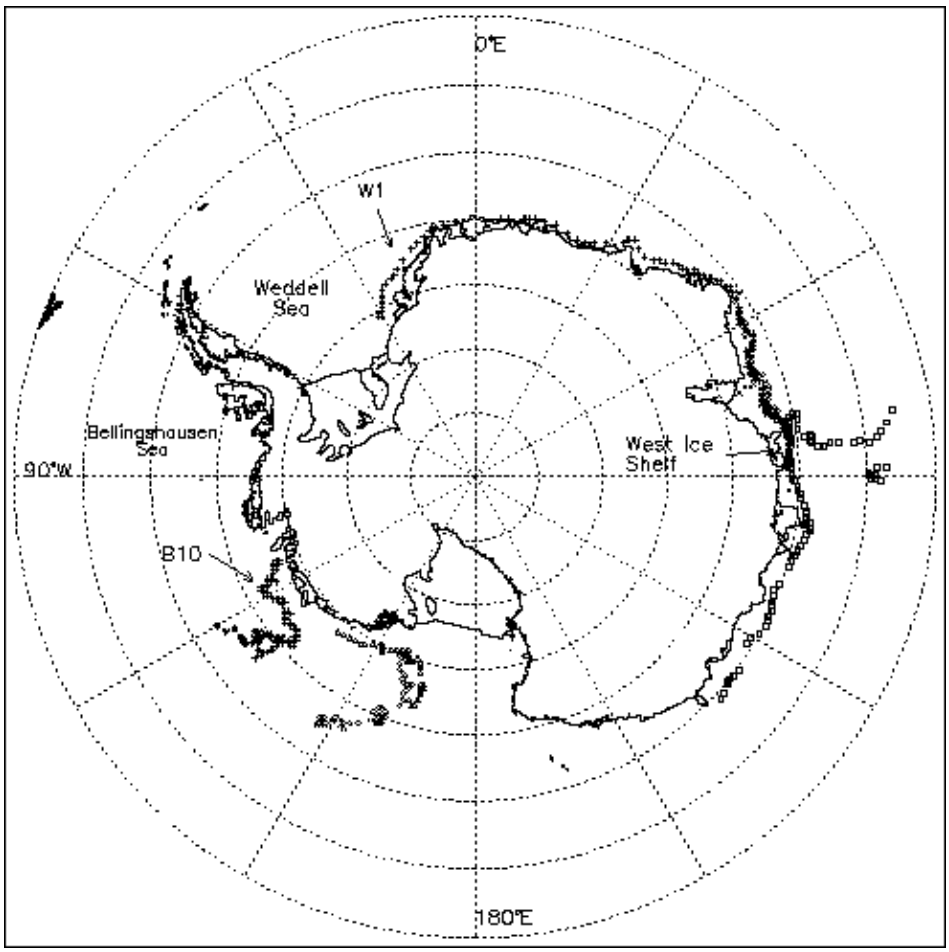

Figure 7. Drift tracks of eight icebergs tracked in the time series of 5-day composite images of normalised backscatter. Close to the coast the sense of the drift is anti-clockwise around the continent with the westward continental slope current (or Antarctic East Wind Drift). Several tracks exhibit a retroflection, a stage with northward drift, then a drift to the east with the ACC [Antarctic Circumpolar Current] (or West Wind Drift).

Conclusions

The generation of an animated sequence of composite radar images of Antarctica provides an ability to visualise the evolution over time of various events. The images show the onset and duration of the effect of surface melting on the moisture content of the snow. Time series of normalised backscatter values for any given point provide detail of the evolution of events and quantitative measures of the effect. The images also clearly show the drift of very large icebergs with the ocean currents. Their tracks provide additional information on the broad scale pattern of the currents about Antarctica. The magnitude of the backscatter from an iceberg depends on the snow surface properties, the effect of melting, and its size. The images provide the longest continuous record of observations for an iceberg using an active microwave instrument, and a method to generate a continuous record of an iceberg's size. Current developments are extending this work to a larger number of icebergs using higher resolution radar systems to infer ocean currents and dissolution rates of icebergs.

Acknowledgements

The ERS (AMI) wind scatterometer data are copyright to ESA, 1991-1996, and provided through AO project ERS.AO2.AUS103. We also wish to acknowledge the efforts and support of the CERSAT team of the French PAF in the production and dissemination of the data products. Davis meteorological data were provided by the Australian Bureau of Meteorology's Antarctic climate centre in Hobart, Australia.

References

Rott, H., H. Miller, K. Sturm & W. Rack 1994:
Application of ERS-1 SAR and scatterometer data for studies of the Antarctic ice sheet. In: Proceedings of the Second ERS-1 symposium, 11-14 October 1993, Hamburg, Germany, ESA Publication ESA SP-361 Vol. 1, pp. 133-139.

Rott, H. & Th. Nagler 1993:
Snow and glacier investigations by ERS-1 SAR - First results. In: Proceedings First ERS-1 Symposium, 4-6 November 1992, Cannes, France, ESA Publication ESA SP-359 Vol 2, pp. 577-582.

Rott, H. & Th. Nagler 1994:
Capabilities of ERS-1 SAR for snow and glacier monitoring in alpine areas. In: Proceedings Second ERS-1 Symposium, 11-14 October 1993, Hamburg, Germany, ESA Publication ESA SP-361 Vol 2, pp. 965-970.

Tchernia, P. & P.F. Jeannin 1980:
Observations on the Antarctic East Wind Drift using tabular icebergs tracked by satellite Nimbus F (1975-1977). Deep-Sea Research, 27A, 467-474.

Tchernia, P. & P.F. Jeannin 1984:
Circulation in Antarctic waters as revealed by iceberg tracks 1972-1983. Polar Record, 22(138), 263-269.

Young, N.W., D. Hall & G. Hyland 1996:
Directional anisotropy of C-band backscatter and orientation of surface microrelief in East Antarctica. In: Proceedings of the First Australian ERS Symposium. University of Tasmania, Hobart, 6 February 1996. COSSA Publication 037, 117-126.

A postscript version of this paper (formatted for A4 or US letter) is available for download from
http://www.antcrc.utas.edu.au/glacio/remote_sensing/publications